

A COMPACT IN-AIR X-RAY DETECTOR FOR VERTICAL BEAM SIZE MEASUREMENT AT ALBA

A. A. Nosych, U. Iriso, ALBA CELLS, Barcelona, Spain

Abstract

An in-air x-ray detector (IXD) was developed for ALBA to study the residual x-rays after traversing copper crotch absorbers. The device prototype is placed in-air after such an absorber, mounted flush with the vacuum pipe. The remaining x-rays (above 120 keV) generate a visible footprint if they impinge upon a sensitive enough scintillator. After unsuccessful testing different screens, we are using a Cerium doped PreLude420 (LuYSiO:Ce) screen, whose the image is observed with a simple optics system mounted on a commercial CCD camera. This measurement allows evaluating the vertical electron beam size with exposure times in the order of 1 second. Similar instruments are used at ESRF and ANKA storage rings. This paper presents the results of the first measurements with IXD (March-July 2014), and describes its potential to be used as a full diagnostics tool for the 3 GeV storage ring of ALBA.

INTRODUCTION

At ALBA, as it is widely used in most 3rd generation synchrotron light sources, the emittance in both planes is measured with the usual pinhole method [1]. However, this only provides a local measurement of the vertical emittance, thus a local measurement of the ver/hor coupling. In order to infer the global coupling, readily available measurements of the vertical beam size are desirable.

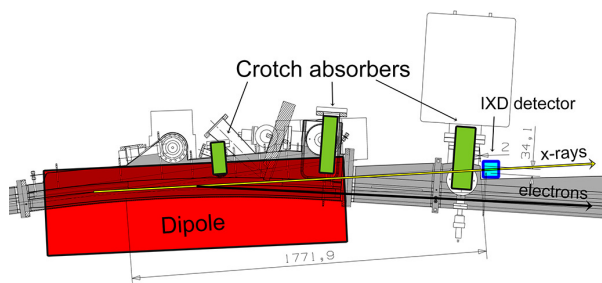


Figure 1: Tunnel section layout, showing a bending magnet with water cooled absorbers and paths of the electron and photon beams.

In-air X-ray Detectors (IXD), developed first at ESRF [2] and ANKA [3], are cheap and simple devices that can provide such measurements. They use the “left-over” hard x-rays produced by the dipoles and going through the absorbers to obtain an image of the synchrotron radiation fan, from where the vertical beam size can be inferred.

At ALBA, the unused excess of x-rays generated by 32 1.4 Tesla dipoles are damped by water cooled absorbers, which are mounted by sets of three into each dipole (Fig. 1). The absorbers are thick large-toothed copper jaws, half-open to

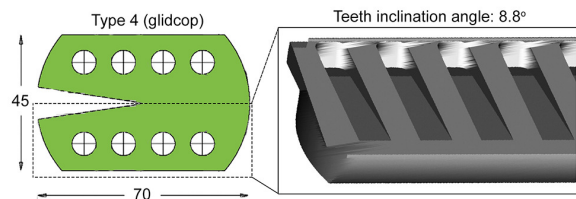


Figure 2: Transverse cross-section of the crotch absorber and a model of its lower jaw.

form a crotch geometry (Fig. 2), with a minimum thickness of 35 mm and are aimed at complicating the path of x-rays traversing through. Only a fraction of low intensity higher-energy flux can penetrate the absorbers; however, if detected, it can serve as an alternative diagnostics tool for real-time monitoring of vertical beam size and emittance.

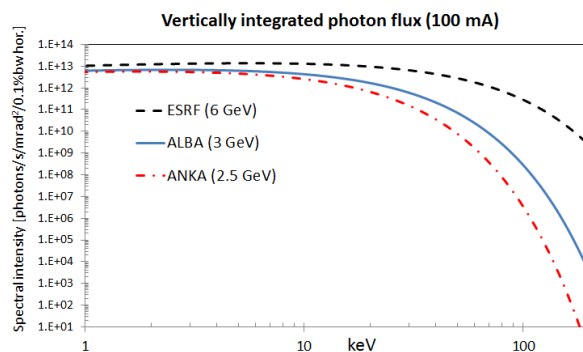


Figure 3: Vertically integrated x-ray spectrum emitted by bending magnets for machines using iXD detectors.

At ESRF and ANKA the combination of beam energy and absorber thickness offer favorable conditions for these detectors: the 6 GeV ESRF has 40 mm absorbers, and 2.5 GeV ANKA has 8 mm absorbers. ALBA is the first 3 GeV 3rd generation synchrotron light source where this technology is applied, which has become possible after choosing the appropriate scintillating material.

The total photon emission, summed over all vertical angles, emitted when an electron beam of energy E crosses a dipole is:

$$N = 2.46 \times 10^{13} E I_b \int_{\frac{\epsilon}{\epsilon_C}}^{\infty} K_{5/3}(u) du \quad (1)$$

in units of photons/second/h-mrad/0.1%BW, where I_b is the electron beam current and $u = \epsilon/\epsilon_C$ is the ratio between the photon energy ϵ and the machine critical energy ϵ_C . For reference, Figure 3 compares this flux to other synchrotron light machines for fixed intensity $I_b = 100$ mA, while Fig. 4

compares the flux remained after traversing an absorber corresponding to each machine.

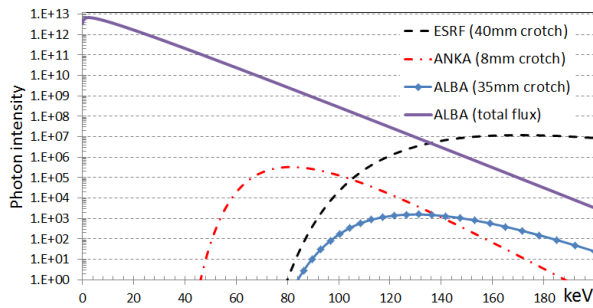


Figure 4: Photon flux before and after traversing crotch absorbers at ALBA (solid lines), compared with the flux after traversing corresponding absorbers at ESRF and ANKA (dashed lines). Note that ALBA flux after the crotch absorber is between 2 and 4 orders of magnitude lower.

DETECTING X-RAYS IN THE AIR

The prototype in-air x-ray detector (IXD) is placed downstream of a 3rd absorber of one of the storage ring dipoles (absorber Type 4 in Dipole 02 of Sector 01), and intercepts the remaining photons after they pass through a minimum of 35 mm of copper and 2 mm of steel anti-chamber wall (Fig. 2).

The IXD consists of a short optics line which provides a 18×14 mm field of view over a 1034×779 px sensor of a commercial Basler Scout CCD camera, and a 0.8 mm thick PreLude420 scintillating screen, which converts the detected x-rays to visible light. We have selected the PreLude material (Cerium doped LuYSiO₅) for its sensitivity to higher energy photons compared to other common scintillators like e.g. CdWO₄ used at ANKA and ESRF (Fig. 5). We also tested the available YAG screens, with unsuccessful results.

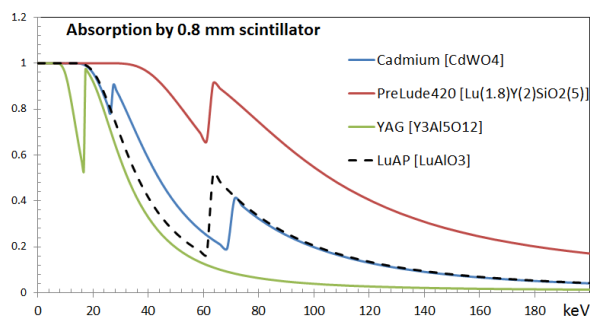


Figure 5: Photons absorption in various 0.8 mm scintillators.

Ray tracing study indicates that IXD observes a part of the x-ray fan corresponding to 4.35° of bending curvature, which is equivalent to a 150 mm arc inside a 1370 mm bending magnet. LOCO simulation (“Linear Optics from Closed Orbit” software) of the electron beam size variation along the magnet (Fig. 6) is fully compatible with the electron

beam size measurement done by the pinhole monitor [1]:

$$\sigma_{y,e}^{\text{loco}} = \sigma_{y,e}^{\text{pinhole}} = 24 \mu\text{m}.$$

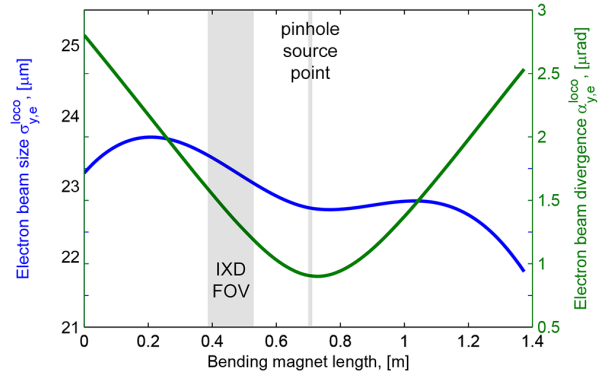


Figure 6: Vertical beam size (mean) and divergence in the considered bending magnet. The gray-highlighted section is the field of view of the IXD (15 out of 140 cm)

The photon source point for the pinhole monitor is located in another sector of the ALBA storage ring, in particular, in the central part of a dipole with identical characteristics to the one used for IXD.

The dipole spectral characteristics before ($\epsilon_{\text{crit}} = 8.5$ keV) and after absorption ($\epsilon_{\text{max}} = 130$ keV) indicate the reduction in total flux of the remaining x-rays by a factor of 10^9 with respect to the initial intensity, see Fig. 4 calculated with XOP [4]. In particular, ALBA’s absorbers reduce the 130 keV flux by a factor of 5×10^5 , luckily, enough to leave a footprint on the PreLude screen.

Under the assumption of a Gaussian symmetric distribution of electrons in the bunch we calculate the vertical angular distribution of the photon radiation as a function of photon energy [5], Fig. 7:

$$\sigma_r = \sqrt{\frac{2\pi}{3}} \frac{1}{\gamma} \frac{\int_{\frac{\epsilon}{\epsilon_c}}^{\infty} K_{5/3}(u) du}{K_{2/3}^2(\epsilon/2\epsilon_c)} \quad (2)$$

and make a first estimation of the photon beam divergence at 130 keV (for $\psi = 0$): $\alpha_{ph} = 30 \mu\text{rad}$, which corresponds to the remaining x-rays after passing through center of the absorber (exactly 35 mm of copper and 2 mm of steel). A more precise value of photon divergence can be derived by integrating the total remaining flux over all energies: $\alpha_{ph} = 25.2 \mu\text{rad}$. An analysis of photon divergence and total transmitted flux as functions of Cu thickness is shown in Fig. 8.

FIRST IXD MEASUREMENTS

Due to low flux and thin PreLude screen, it is difficult to reach sub-second response of the IXD with quantitative results. A typical acquired image with a 10 second exposure time is shown in Fig. 9. The background noise can be removed by subtracting the image acquired at 10 seconds without beam (darkness).

Several unexpected observations were carried out from the first experiments. Firstly, a noticeable tilt (around 1°)

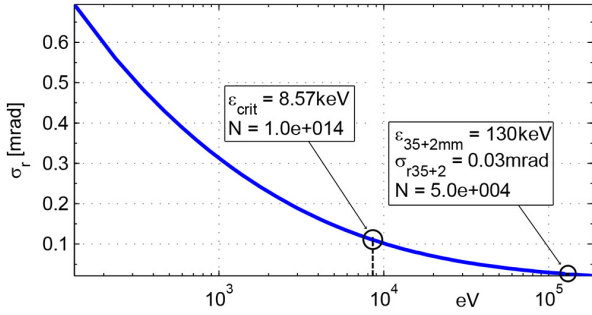


Figure 7: A plot of σ_r versus $\frac{\epsilon}{\epsilon_c}$ for ALBA beam.

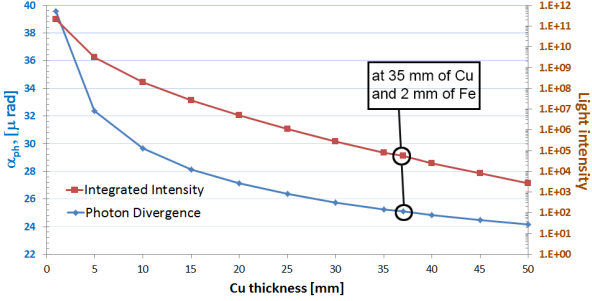


Figure 8: Relation between integrated flux transmission and photon divergence as functions of Cu thickness.

of the photon imprint can be explained by inaccuracy of camera alignment done by hand, or the vertical beam orbit variation within the 150 mm length of the observed dipole arc.

Secondly, the photon beam is observed with spots of different intensities. These can not be related neither to cooling tubes inside the absorbers (they are located below and above the photon beam), nor by the fan from upstream bending. However, they can be explained by the design of the absorber and its “teeth”, in particular in the path of the x-rays: the more intense part of the beam traverses less copper. An indication of this can be the fact that the gap of 6 mm of least light intensity in the central part of the IXD image corresponds to the 6 mm width of a “tooth” (Fig. 2).

Lastly, by measuring the vertical photon beam size in Fig. 9 in three different regions of the fan we obtain a value of around $\sigma_{y,ph}^{ixd} = 70 \mu\text{m}$. By deconvoluting it down to vertical electron beam size we obtain a value of

$$\sigma_{y,e}^{ixd} = \sqrt{(\sigma_{y,ph}^{ixd})^2 - R^2(\alpha_{ph}^2 + \alpha_e^2)} = 56 \mu\text{m}, \quad (3)$$

where $\alpha_e = 1.6 \mu\text{rad}$ is the theoretical electron beam divergence in the considered dipole. The explanation to the factor of 2.3 difference between $\sigma_{y,e}^{ixd}$ and both $\sigma_{y,e}^{pinhole}$ and $\sigma_{y,e}^{loco}$ is yet to be found. The focus of the study is on a possible optical effect, created by elements in the x-ray path, i.e. an underestimation of copper thickness and photon scattering inside copper itself.

The IXD images obtained within 10 to 1 second exposure times measure identical photon beam size. At sub-second

shutter speeds the central part of the beam imprint (with least intensity) saturates in the background noise.

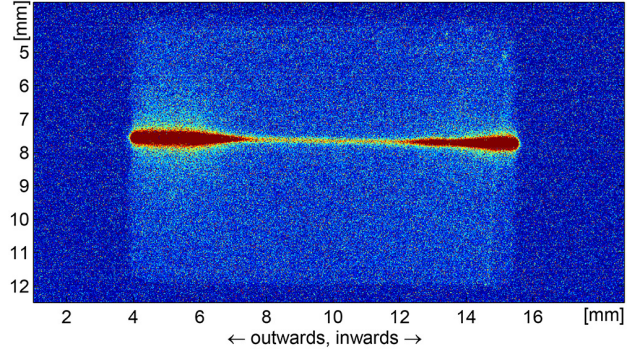


Figure 9: IXD images with and without background, for 10 and 1 sec exposure.

BEAM SIZE TESTS

As part of a beam test, the IXD vertical photon beam size $\sigma_{y,ph}^{ixd}$ was calibrated against the vertical electron beam size by the pinhole $\sigma_{y,e}^{pinhole}$ while changing the beam coupling. The coupling factor κ (vertical to horizontal emittance ratio) was increased to 1.28% and decreased to 0.3% from the nominal value of 0.5%. It can be seen that at low coupling the photon beam size (red curve) measurement saturates, while the pinhole (blue curve) remains highly sensitive to small beam size changes. This measurement makes it possible to evaluate experimentally the α_{ph} to better understand the uneven photon imprint on the IXD screen.

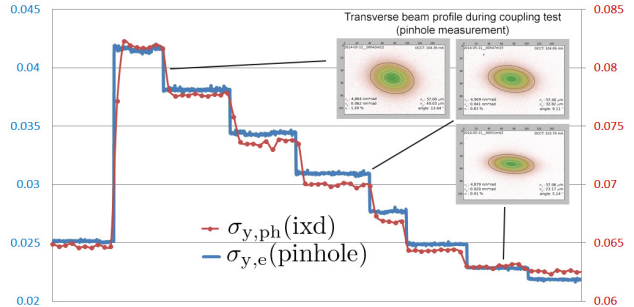


Figure 10: Calibrating vertical photon beam size against the electron beam size.

CONCLUSIONS

We have successfully developed and tested an in-air x-ray detector which measures the vertical photon beam size from the flux remaining after traversing the copper absorbers. The measurement results reveal the full potential of IXD to become a promising powerful diagnostics tool for the ALBA storage ring.

The limits of its application and several uncertainties were identified, e.g. a “tooth-shaped” fan profile and the electron beam size discrepancy with theoretical value, which will

be investigated and improved. Currently the tests are ongoing with scintillating screens of different materials (e.g. CRY19) and thicknesses to reach sub-second response time and higher output light intensity.

We are also looking into Fluka/Penelope simulations of photon scattering in copper to verify its role in changing photon divergence, which could explain the photon fan profile.

ACKNOWLEDGMENTS

We would like to thank the ALBA Computing, Engineering and Experiments divisions, in particular S. Blanch, J. Montero and I. Sics for all invaluable assistance, Z. Marti and M. Quispe for LOCO calculations and ray tracing, and K.B. Scheidt of ESRF for important discussions and advise.

REFERENCES

- [1] Beam size and emittance measurements using the ALBA Pin-hole, U. Iriso, ALBA Project Document No. AAD-SR-DI-PINH-01, 2011.
- [2] Detection of hard x-rays in air for precise monitoring of vertical position and emittance in the ESRF dipoles, B. K. Scheidt, Proc. DIPAC-2005, pp. 238-240, 2005.
- [3] Precise measurements of the vertical beam size in the ANKA storage ring with an in-air x-ray detector, A.-S. Mueller, I. Birkel, E. Huttel, P. Wesolowski, Proc. EPAC-2006, pp. 1073-1075, 2006.
- [4] X-ray Oriented Programs (XOP 2.3), www.esrf.eu, 2014.
- [5] The science and technology of undulators and wigglers, James A. Clarke, Oxford Publications, 2004.